DIFFRACTION OF ELECTROMAGNETIC WAVES AT MICROWAVE FREQUENCIES

Thesis for the Degree of M. S.

MICHIGAN STATE UNIVERSITY

Fr. Jules A. Boucher

1956

PLACE IN RETURN BOX
to remove this checkout from your record.
TO AVOID FINES return on or before date due.

DATE DUE	DATE DUE	DATE DUE

DIFFRACTION OF ELECTROMAGNETIC WAVES AT MICROWAVE FREQUENCIES.

By

Fr. Jules A. Boucher.

A THESIS

Submitted to the College of Science and Arts of
Michigan State University of Agriculture and
Applied Science
in partial fulfillment of the requirements for the degree of
MASTER OF SCIENCE.

Department of Physics.

-1956-

7-25-56
9

RECONNAISSANCE.

Je désire, dès maintenant, exprimer toute mon appréciation pour l'aide précieuse et les suggestions innombrables que le Professeur C.D.Hause a bien voulu me fournir tout au long de ce travail. De même, l'intérêt des autres membres de la faculté n'a pas été sans porter encouragement.

Jules A. Boucher, ptre

TABLES OF CONTENTS.

INTRODUCTION.

The problem of diffraction of electromagnetic waves has attracted the interest of many investigators of all types, from the theoretician to the experimentalist. Until recent years, the work was confined almost entirely to optical frequencies and apertures, and observation distances large in comparison to the wave length. The greatest difficulties were then of two kinds:

1) The irreducible gap between the ideal case, which can be treated theoretically, and the physical situation.

2) The absence of electromagnetic waves of suitable wavelength. The available waves were either too short or too long to permit a practical study of all aspects of diffraction.

But now that we can produce microwaves, the second difficulty disappears. The problem we are left with is the realization of experiments as close as possible to the ideal case.

Our purpose then is to observe and explain semi-quantitatively several diffraction patterns of 12. cm. microwaves produced by slit apertures. The observations are made in the neighborhood of the apertures, at distances not exceeding several wavelengths. A qualitative explanation of the observed patterns is obtained by using Thomas Young's method of interpretation. The patterns are represented as being formed by the interference of the direct wave and secondary waves which arise at the edges of the apertures.

A more quantitative account is obtained by comparing our data with that expected from the exact treatement by Sommerfeld (1) of the diffraction by an infinite half-plane. Application of this theory to our problem is only partially valid and discrepancies are expected.

OUTLINE OF THEORY.

Our interest in this field was excited by an article in "The Physical Review" (2), where C.L. Andrews studies quite extensively the diffraction of 12cm. microwaves by a circular aperture. That work presents the patterns in the H-plane as well as in the E-plane, thus stressing the differences.

Andrews does not extend his observations to the geometrical shadow, and being three-dimensional, the quantitative interpretation of his readings is made more complicated and the qualitative interpretation is not helped. We will limit ourselves to a two-dimensional study, and, at the same time, we will observe only in the H-plane. However, the high degree of polarization shown by our apparatus would provide facilities also for good readings in the E-plane. We will indicate later the small differences due to the absence of a third dimension.

Andrews himself, in a later paper (3), does not hesitate in pointing out that "in the plane of the aperture, ..., Young's theory yields the experimentally observed positions of maxima and minima".

In this work, we will also attempt to account for maxima and minima even in the geometrical shadow.

Another investigator, Houston (4), successfully detected a "turn up" effect near the edge of a diffracting aperture, indicating the correctness of the predictions of electromagnetic theory.

Houston was using a long wavelength (50 cm.), and the patterns are similar in general to those obtained by Andrews. We are unable to detect close edge effects in our readings for two reasons:

a) We are using a shorter wavelength. The detector is relatively large in comparison to the wavelength, approximately 0.1λ.

b) The edges of the apertures are not thin and knife-like, which is the primary condition to get those effects.

The problem of diffraction of a plane wave by a conducting half-plane has been solved by Sommerfeld. The disturbed field takes on three different forms, each having its own equation:

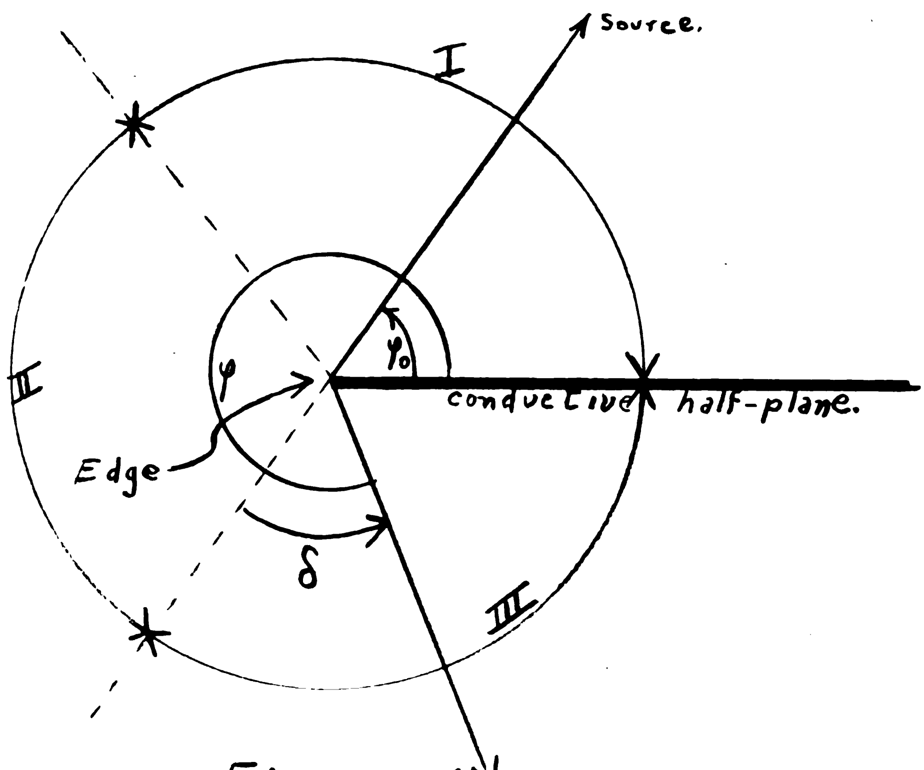

Figure:1

In the region number I, called the reflection region,

we can represent the disturbed field by the equation:

$$U_{\pi,\sigma} = \cos[Kr\cos(\varphi-\varphi_0)] \mp \cos[Kr\cos(\varphi+\varphi_0)] + Z$$

where the first term on the right is the incident plane wave, and the next term is the reflected plane wave.

In the region number II, called the unshadowed region, we can represent the disturbed field by the equation:

$$U_{\pi,\sigma} = \cos[Kr\cos(\varphi-\varphi_0)] + Z$$

In the region number III, called the shadow region, we can represent the disturbed field by the equation:

$$U_{\pi,\sigma} = Z = \frac{1}{4\pi}\sqrt{\frac{\lambda}{r}}\left[\cos(Kr+\pi/4)\right]\left[\pm\frac{1}{\cos\left(\frac{\varphi+\varphi_0}{2}\right)} - \frac{1}{\cos\left(\frac{\varphi-\varphi_0}{2}\right)}\right]$$

In all these equations, the term Z is a cylindrical wave arising at the edge, and K is the propagation constant $\frac{2\pi}{\lambda}$. It can be shown that the cylindrical wave arising at the edge undergoes a phase change of 180°, when the angle $\varphi-\varphi_0$ goes from $\varphi-\varphi_0<\pi$ to $\varphi-\varphi_0>\pi$

And, because of the term $\frac{\pi}{4}$ in the wave function, we will have an inflected wave differing from the undisturbed wave by an angle $\frac{\pi}{4}$, when $\varphi-\varphi_0>\pi$, or a deflected wave differing from the undisturbed wave by an angle $\frac{5\pi}{4}$, when $\varphi-\varphi_0<\pi$.

In the case we will be dealing with, φ_0 is equal to $\pi/2$ and the E-field is parallel to the slit (π case). In this present case, (see Fig. 2), the above formula for a cylindrical wave, transforms into:

$$Z_\pi = \frac{1}{4\pi}\sqrt{\frac{\lambda}{r}}\left[\cos(Kr+\pi/4)\right]\left[\frac{-1}{\cos\delta/2} + \frac{1}{\sin\delta/2}\right]$$

where δ is the angle between the radiation and the normal n, and where $\sqrt{\frac{\lambda}{r}}$ may be called the distance factor, and $\left[\frac{-1}{\cos\delta/2} + \frac{1}{\sin\delta/2}\right]$

is an angle factor.

It is to be noted that the above formula does not apply in the neighborhood of $\delta = 0$. Here, we are on the edge of the shadow, and also, the cylindrical wave changes phase.

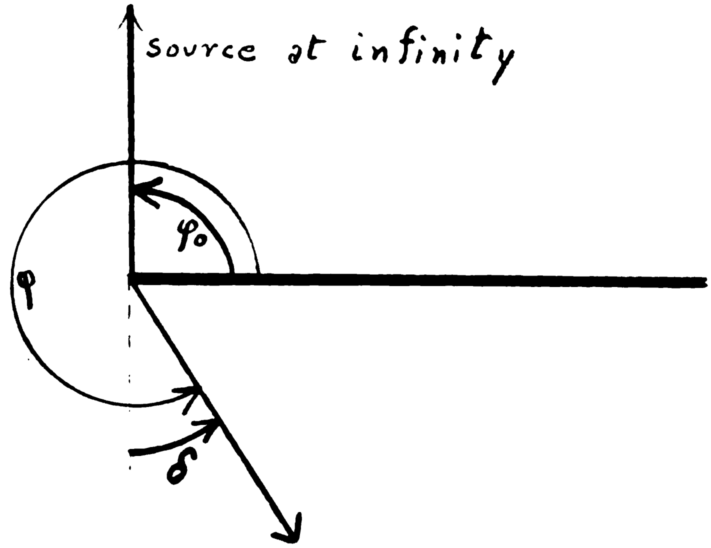

Figure: 2

n

Young's interpretation of diffraction patterns can be shown from the following:

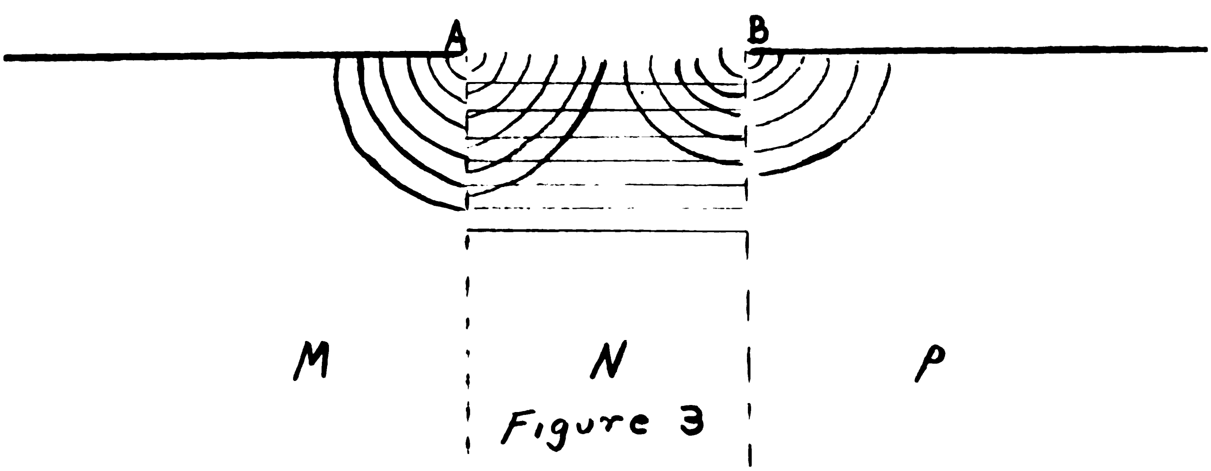

Figure 3

Consider regions M, N, P.

In M, we have interference of the inflected wave from A and the deflected wave from B. In N, we have interference of the deflected waves from A and B, and the plane wave from the source at infinity. In P, we have interference of the deflected wave from A and the inflected wave from B. In the plane of the slit, we have a special case of N.

It is apparent that Young's interpretation can be made semi-quantitative by assuming two Sommerfeld half-planes slightly separated and the edges giving rise to the inflected and deflected cylindrical waves.

We do not expect complete agreement for the following reasons:

1) The slit is not an "infinite" one.

2) Each half-plane is not infinite.

3) The slit jaws are close enough to each other to interact with each other.

4) The edges are not knife-like.

5) The"plane wave" is plane in two dimensions only instead of three as required by Sommerfeld's Theory.

THE PRODUCTION OF A PLANE WAVE AT MICROWAVE FREQUENCIES.

A) The generator.

We were fortunate enough to be equipped with a microwave generator fullfilling all the requirements one can ask for: stability, power, portability, etc. That generating unit is a Microwave Diathermy Generator, commercially known as "Microtherm" and manufactured by Raytheon Manufacturing Company, Waltham, Mass. The model used in this experiment was the CMD-4, Series A-1425.

The "Microtherm" operates at a frequency of 2450 Mc., or a wavelength of 12.2 cm. Its energy is generated in a continuous-wave magnetron oscillator. The unit has a power output of at least 100 watts.

A diagram of the main components of this unit appears in Fig. 4

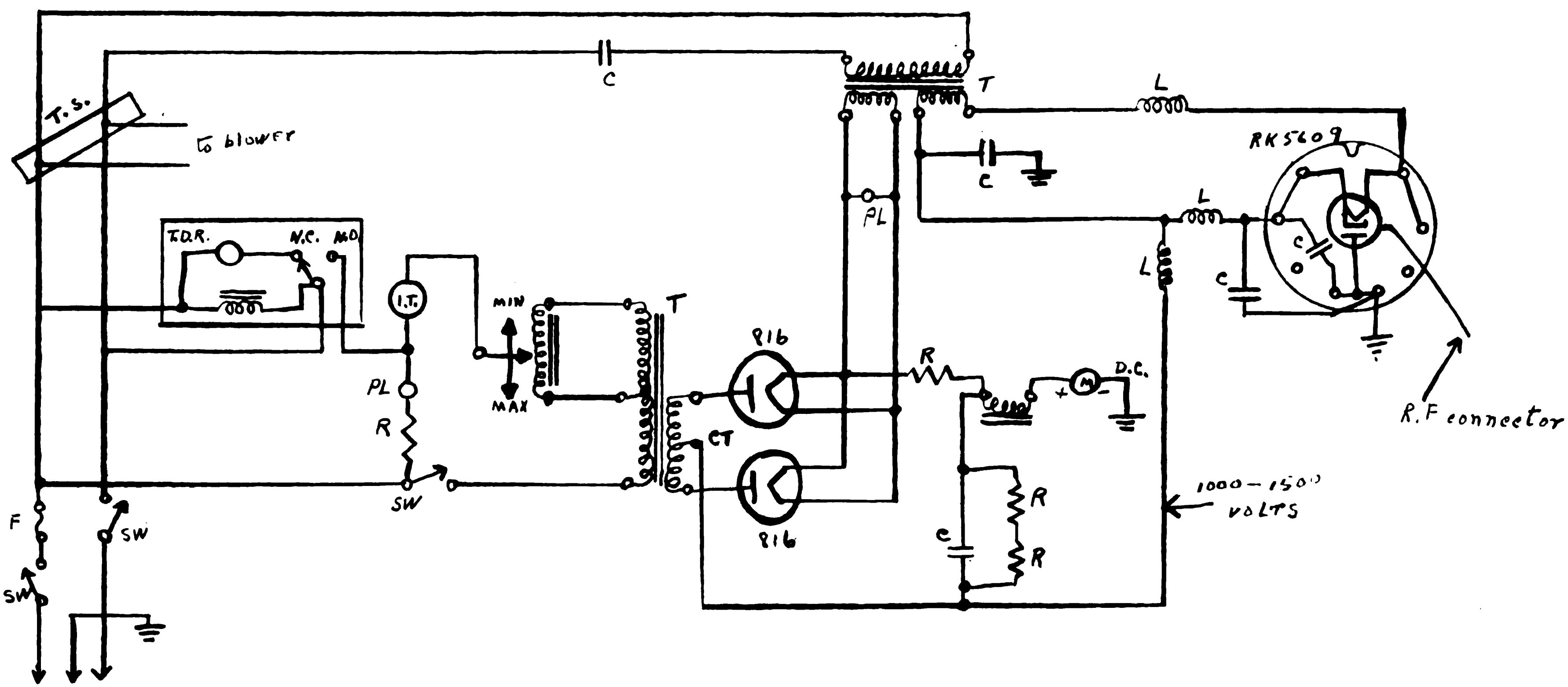

T.S.
To blower
T.D.R.
N.C.
N.O.
I.T.
PL
R
SW
F
SW
SW
MIN
MAX
T
816
816
CT
C
T
L
C
PL
R
D.C.
+
-
R
R
C
L
L
C
RK5609
C
R.F connector
1000–1500 VOLTS

Figure 4

B) The reflector and its feed.

The reflector: Since we intended to work in two dimensions only instead of three, we used a parabolic cylinder as a reflector. In so doing, the reflected wave is a plane wave in the horizontal plane.

The reflector is about one meter wide and one meter high. The distance from the focus to the directrix of the parabola is four wavelengths: 48.8 cm. The parabolic cylinder was first made of wood and then coated with aluminum foil. Evidently, this aluminum surface is far from being perfect but irregularities are less then one tenth of a wavelength, so that they could be neglected.

In a parabolic cylinder, the focus is a line, so that we can "feed" it from anywhere on that line.

And, for a reason to be explained later, we thought better to have the upper portion of the reflector larger than the lower. The feed was installed in the lower part of the focus.

Its feed: This was of the dipole-disk type, for these reasons:

a) We wanted as much reflection as possible on the parabolic cylinder and the dipole-disk type shows a good directivity as can be seen from Fig. 6a

b) We wanted to avoid interference between the reflected wave from the reflector and the direct radiation from the feed. This requirement is fullfilled nicely by the dipole-disk feed.

Now, as can be noticed from Fig. 6b, the E-plane distribution of intensity is asymmetrical. This is due to the asymmetry of the dipole. This is the reason why we used an asymmetrical position for the feed. But this minor inconvenience turned out to be

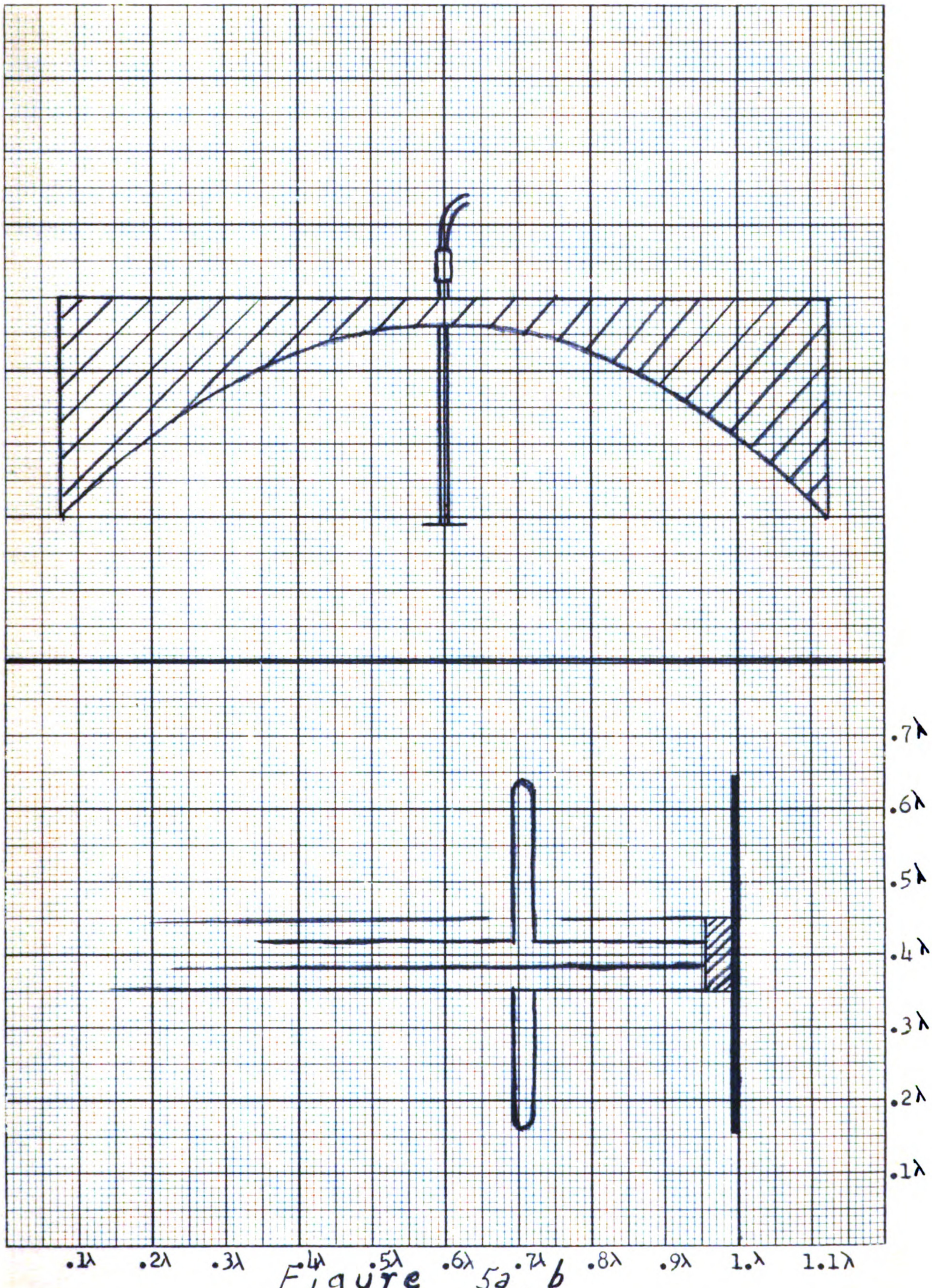

Figure 5a, b

an advantage, since we avoid a "shadow" of the feed in our wave field.

Fig. 5b gives an idea of the different dimensions of the dipole-disk feed. All the different parts of the feed were made of brass.

C) The detector:

The detection ensemble here approximates a point detector. For that reason, as a probe or "antenna" we used the detector itself: a 1N23 crystal. And furthermore, that crystal proved to be quite sensitive to polarization. It is interesting to note that, since we were observing in the H-plane only, the length of the crystal did not matter at all.

The crystal was connected by a pair of twisted wires to an ammeter. The readings of the ammeter were directly proportional to the intensity of the radiation.

D) The field at 520 and 550 cm. from the reflector.

If everything were perfect, the radiation obtained should be collimated in the horizontal plane, and also the intensity should be uniform.

In Fig. 7 , we have plotted the intensity of the field at 520 and 550 cm. from the reflector. As can be seen from the two graphs, the field did not vary by more than 4% either side of an average, over a 60 cm. range.

Those two distances of 520 and 550 cm. were chosen since they were the positions of the diffracting aperture and field plane for the majority of measurements.

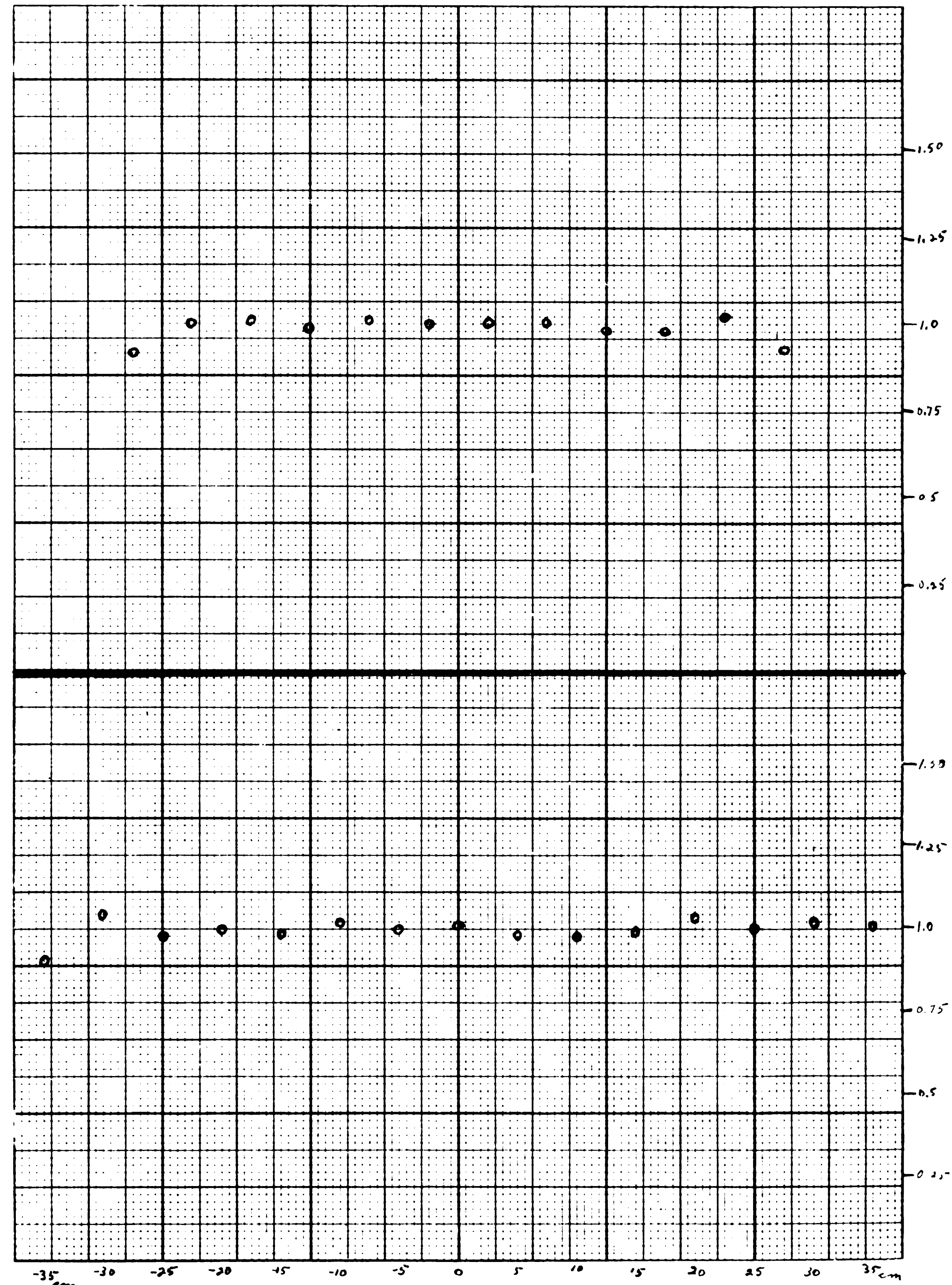
1.50
1.25
1.0
0.75
0.5
0.25
1.50
1.25
1.0
0.75
0.5
0.25
-35 cm
-30
-25
-20
-15
-10
-5
0
5
10
15
20
25
30
35 cm

Figure 7

E) Wavelength in paraffin and index of refraction of paraffin.

To determine the index of refraction of paraffin at 2450 Mc., a cylindrical lens of paraffin was constructed, its focal length measured at this frequency and the index deduced.

The cylindrical lens was of the plano-convex type.

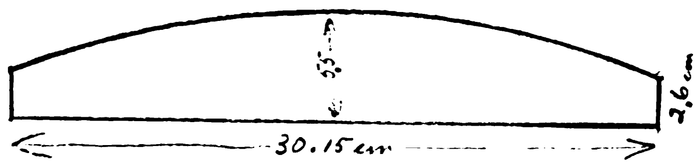

Figure 8

The essential dimensions of the lens are indicated in Fig. 8 . The radius of curvature of the cylindrical surface is 40.6 cm.

It is known that this type of lens will not have a point focus, because of aberrations and other physical difficulties. But we are certain that the focal point will be indicated by a maximum intensity. Our task is then reduced to a measurement of that intensity.

Measured on three different occasions, the focal line was determined as being 29.3 cm. from the plane surface, the convex surface being turned towards the source, to minimize aberrations.

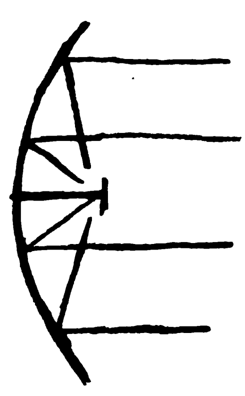

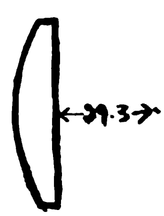

Figure 9

Using thick lens theory, the actual focal length as measured from the principal plane is given by:

$$(1) \quad \frac{1}{f} = (n-1)\left(\frac{1}{R_1} - \frac{1}{R_2} + \frac{(n-1)\,d}{n R_1 R_2}\right)$$

where d is the thickness of the lens.

The positions of the principal planes are given by:

$$(2) \qquad h_1 = \frac{-R_1 d}{n(R_1 - R_2) - (n-1)\,d} \qquad , \quad h_2 = \frac{R_2 d}{n(R_1 - R_2) - (n-1)\,d}$$

For $R_2 \to \infty$, $h_1 = 0$ and h_2 is not determined, but:

$$\frac{d(h_2)}{dR_2} = -d/n$$

so that: (2a) $\quad h_{2_{R_2 \to \infty}} = -d/n$

Now, if we call C the distance from the plane surface to the focus:

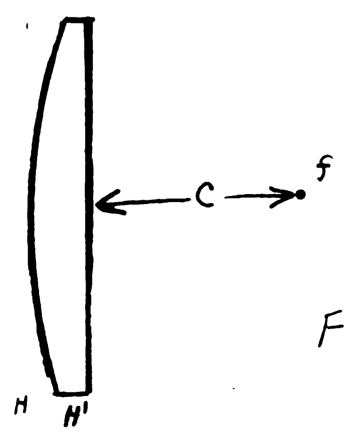

Fig. 10

using equations (1) and (2a), for $R_2 \to \infty$, we obtain

$$(3) \quad \frac{R_1}{n-1} - \frac{d}{n} = C \quad \text{where} \quad \begin{aligned} R_1 &= 40.6 \text{ cm} \\ d &= 5.5 \text{ cm} \\ C &= 29.3 \text{ cm} \end{aligned}$$

Solving for n, the index of refraction at 2450 Mc.

$$29.3\,n^2 - 64.4\,n - 5.5 = 0$$

and n = 2.28

Kittel (5) lists the index of refraction of paraffin at 25,000 Mc. as 2.26

DIFFRACTION OF A PLANE WAVE BY A SLIT WITH CONDUCTIVE JAWS.

A) The slit aperture.

The ideal here would be an "infinite slit" or rather, two infinite conductive half-planes. The best we could do was to set two sheets of thin aluminum alloy in a wooden frame. Each piece was 36 inches high and 6 feet wide. In cases of small widths, this slit would be considered almost infinite.

B) In the plane of the slit:

In Fig. 11, one can see a plot of the intensity distribution accross the aperture of a 2 λ slit, in the plane of the slit. The remarkable features of the pattern are: two maxima at one half of a wavelength from the edge and a minimum in the center. The intensity at the maximum reads 1.78 if one takes as unity the intensity of the undisturbed field. At the minimum point, the intensity reads 0.7 . The amplitude of these two points are 1.334 and 0.836 respectively, unity being again the amplitude of the undisturbed field.

Let us find the amplitude at these two points assuming an infinite slit and applying Sommerfeld's Theory. Let us first take the central point. There the distance from the edge is unity (in units of λ) and the radiation from each of the edges has an amplitude of

$$\frac{1}{4\pi}\left(\frac{-1}{\cos 45^\circ} - \frac{1}{\sin 45^\circ}\right) = \frac{-\sqrt{2}}{2\pi}$$

And since these two radiations are in phase and of equal amplitude, their sum will be just twice: $\frac{-\sqrt{2}}{\pi} = -.45$

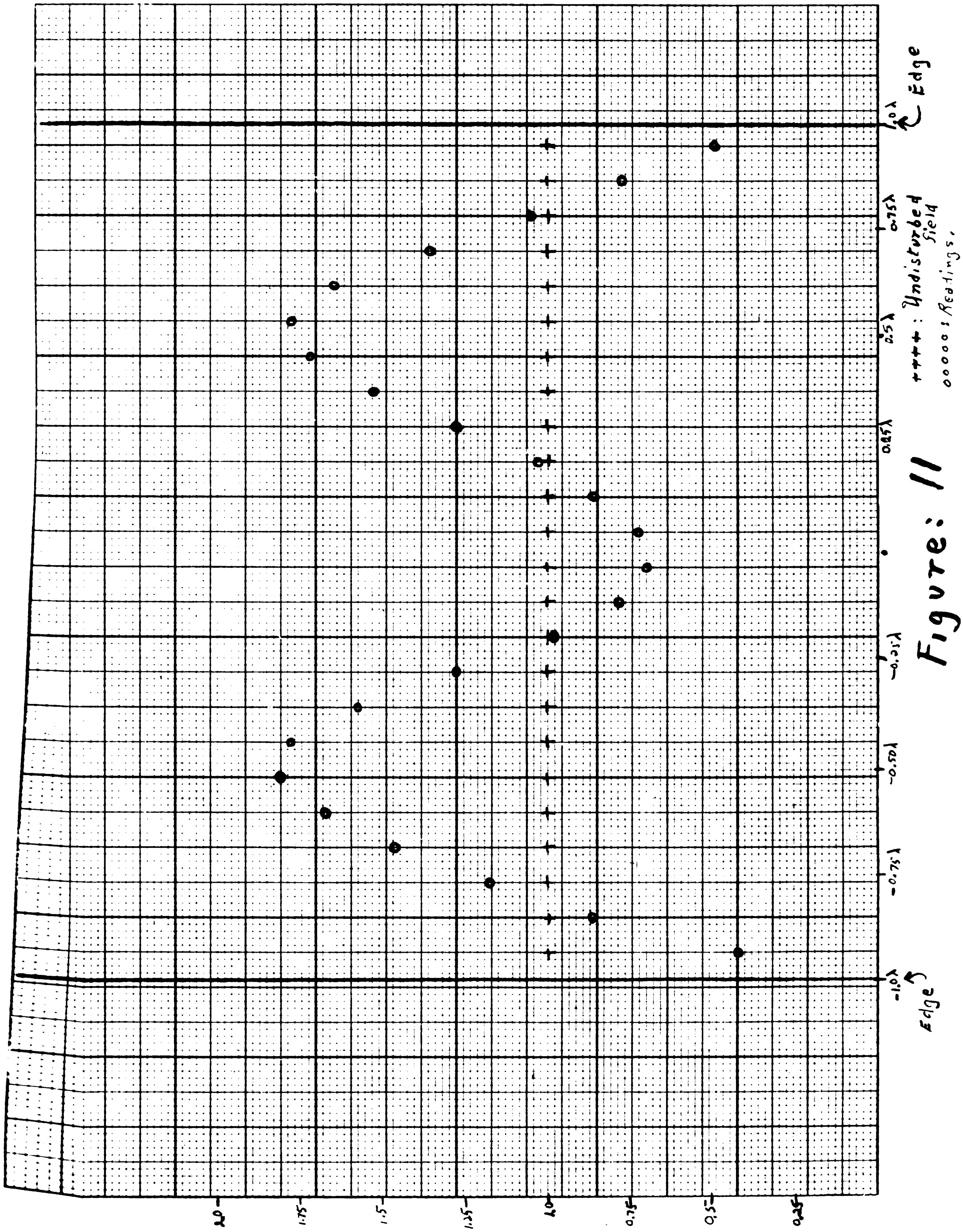

Edge
1.0λ
0.75λ
0.5λ
0.25λ
-0.25λ
-0.50λ
-0.75λ
-1.0λ
Edge
++++ : Undisturbed field
ooooo : Readings.
2.0
1.75
1.5
1.25
1.0
0.75
0.50
0.25

Figure: 11

And remembering that this amplitude has a phase angle of $\frac{5\pi}{4}$ with the radiation from the source at infinity,

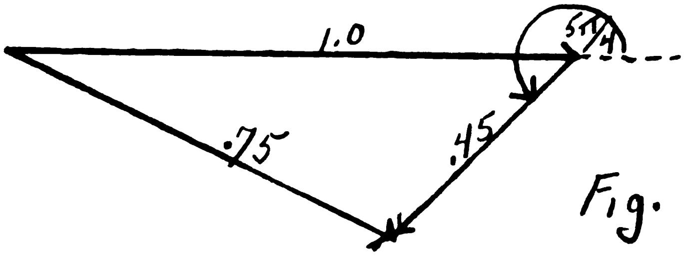

Fig. 12

the resultant amplitude is 0.75 (compared with the measured 0.836). The difference should not be surprising for the reasons explained in the second section. We feel that the major variation is caused by the interaction of the two edges.

Following the same method, one can also get an idea of what the amplitude of the maxima should be. It is to be noticed that here the intensities contributed from the two edges are not equal on account of the different distances of the "sources". The phase angle between these two however remains zero. One can easily figure out that the amplitude of the contribution of the two edges together is $0.519 + 0.181 = 0.5$ and that the phase angle of this amplitude with regard to the radiation from the source at infinity, is $\pi/4$. Then the resultant of all three radiations is:

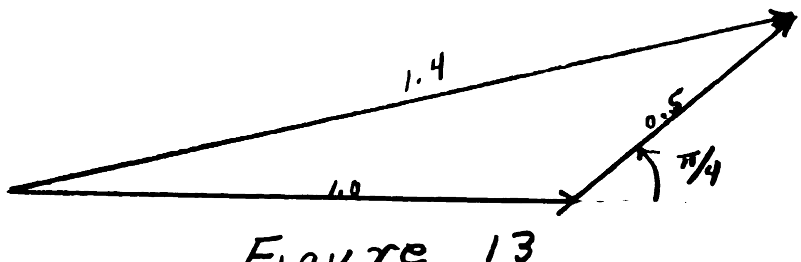

Figure 13

which is an amplitude of 1.4 (compared with the measured 1.334)

Here, it seems interesting to point out that, in the corresponding experiment with a circular aperture, (instead of a slit) Andrews' minimum intensity is practically zero at a point where, with a slit, it is expected to be around 0.56 . And here again, that is not surprising since the two apertures are essentially different.

The jaws of the slit can be opened to any desired width. If the width is three wavelengths, the intensity distribution is that shown in Fig. 14 We have three maxima instead of two. In the present case, let us note that the central maxima is not quite as high as the two lateral ones.

This is to be expected, for, one can go through the same calculations as before and predict that the three maxima will have amplitudes of:

1.36---------1.24---------1.36

and the two central minima will have amplitudes of:

0.78----------0.78

Our readings for the same cases were:

the maxima: 1.26----------1.17----------1.2

the minima: 0.82----------0.71

(Our pattern lacks symmetry but this should not disturb our study). Once more, Andrews' minima go to much lower values because

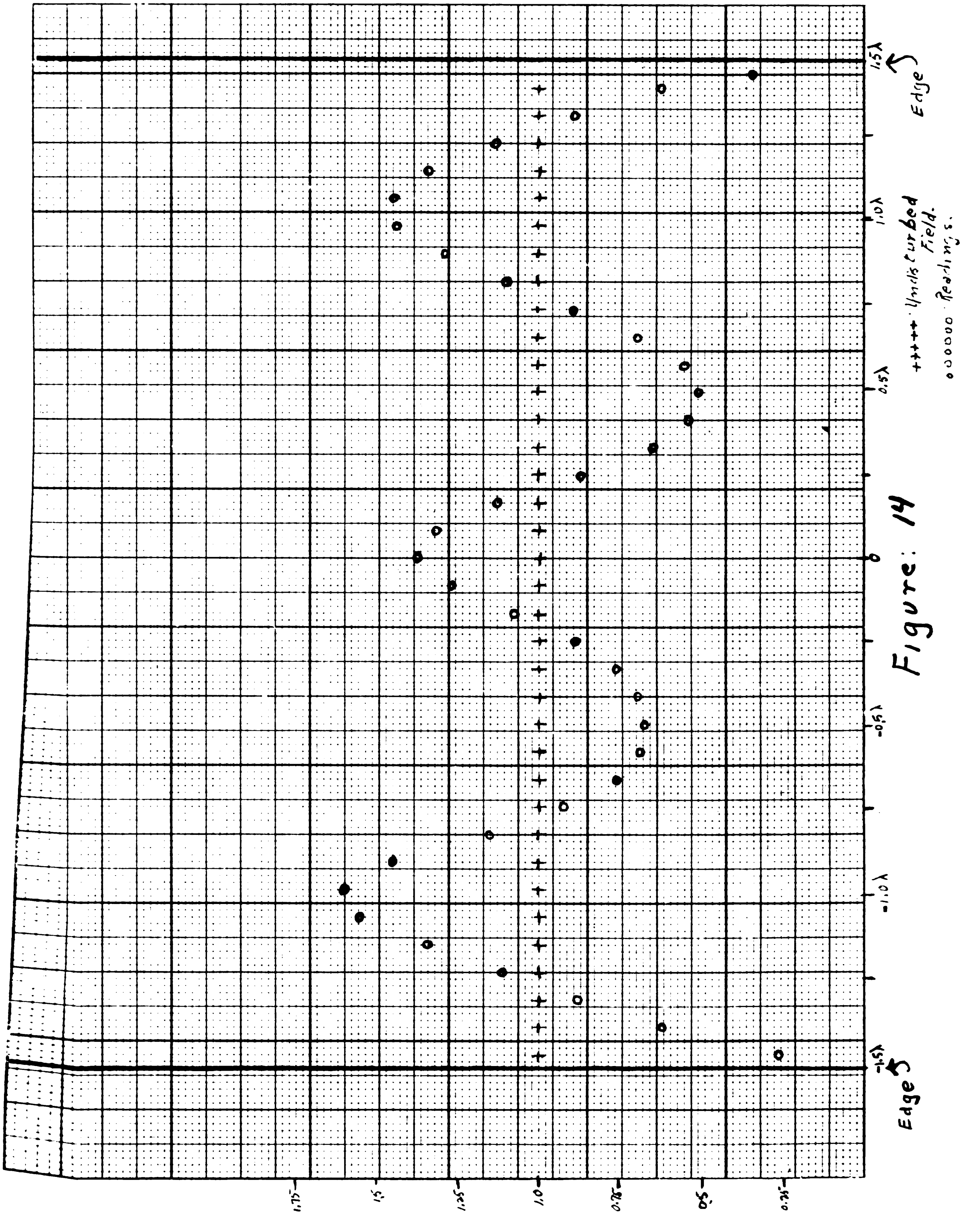
++++ Undisturbed Field.
oooooo Readings.
Edge
Edge
1.5λ
1.0λ
0.5λ
0
-0.5λ
-1.0λ
-1.5λ
1.75
1.5
1.25
1.0
0.75
0.50
0.25

Figure: 14

his aperture is essentially different.

In general then, for a slit width of an integral number of wavelengths, we should expect an equal number of maxima, the weakest in the center, the strongest adjacent to the slit edges.

C) Diffraction patterns near the slit:

Another series of diffraction patterns can be obtained close to the slit.

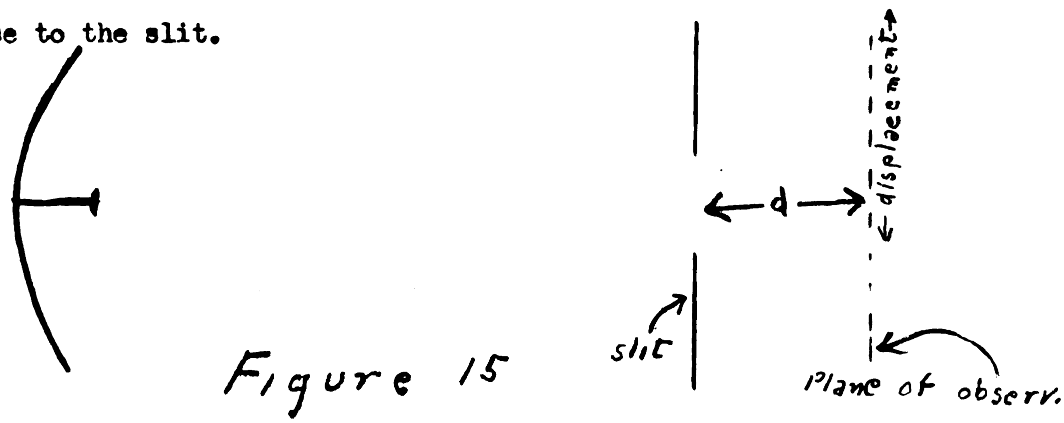

Figure 15

Here again we will forget about a third dimension, and the distance we will refer to will be the distance d, the displacement along the observing plane.

We will study three different patterns: two at a distance of 2.5 wavelengths and one at a distance of 5.0 wavelengths. For the first two, the width of the slit is two and three wavelengths.

The interesting feature of these different patterns is the portion extending into the geometrical shadow. As a matter of fact, according to the interpretation we have followed so far, that portion of the pattern is contributed to by the two cylindrical waves arising at the edges only.

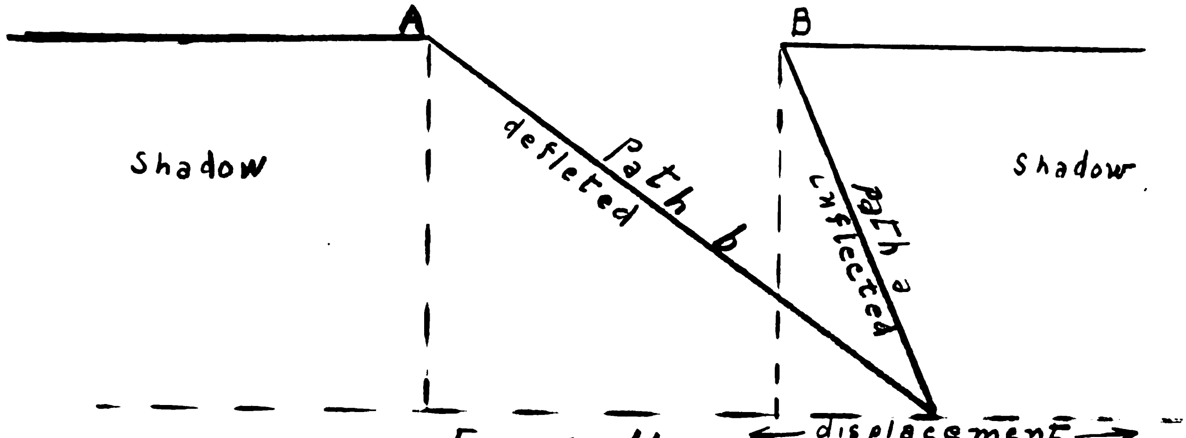

Figure 16

Evidently, a maximum intensity in that region should show up at a point where the two cylindrical waves are in phase. (A small correction for the distance factor $\sqrt{\frac{\lambda}{r}}$ is here neglected). One should not forget that in the shadow region, of the two radiations, one is deflected and the other is inflected. We can say that when the path difference is a half-integer of a wavelength, the two radiations will be in phase, accounting for the phase angle between an inflected and a deflected wave.

In Fig. 18 , we have plotted the intensity distribution at a distance of 2.5 wavelengths, the width of the slit being 2.0 wavelengths.

The maximum point in the shadow region arises in the neighborhood of three wavelengths from the central point. As can be checked easily, the difference between path a and path b at that point is very close to 1.5 wavelengths.

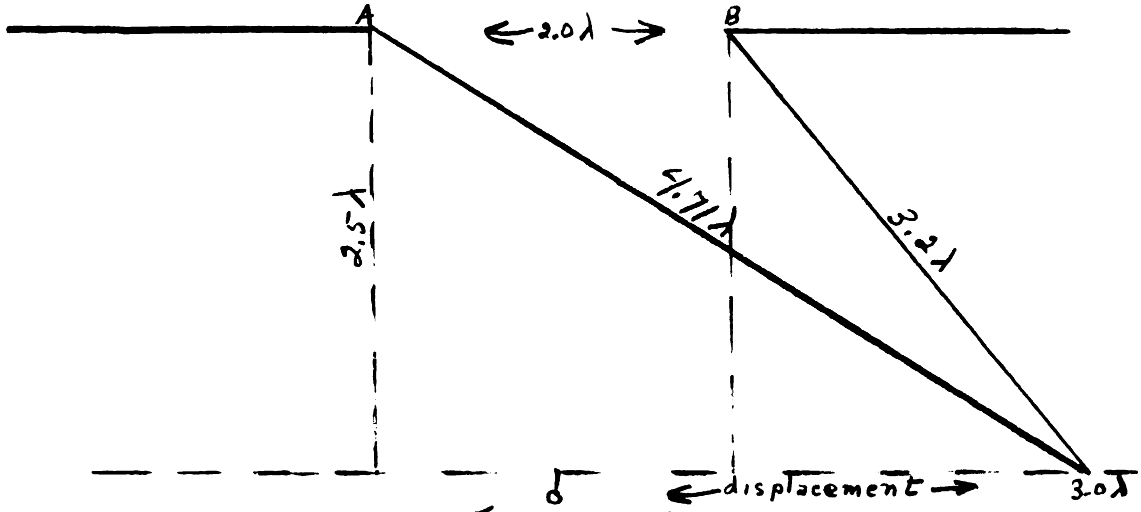

Figure 17

Following the same method, one can verify that at 1.5 wavelength from the central point, where the difference between

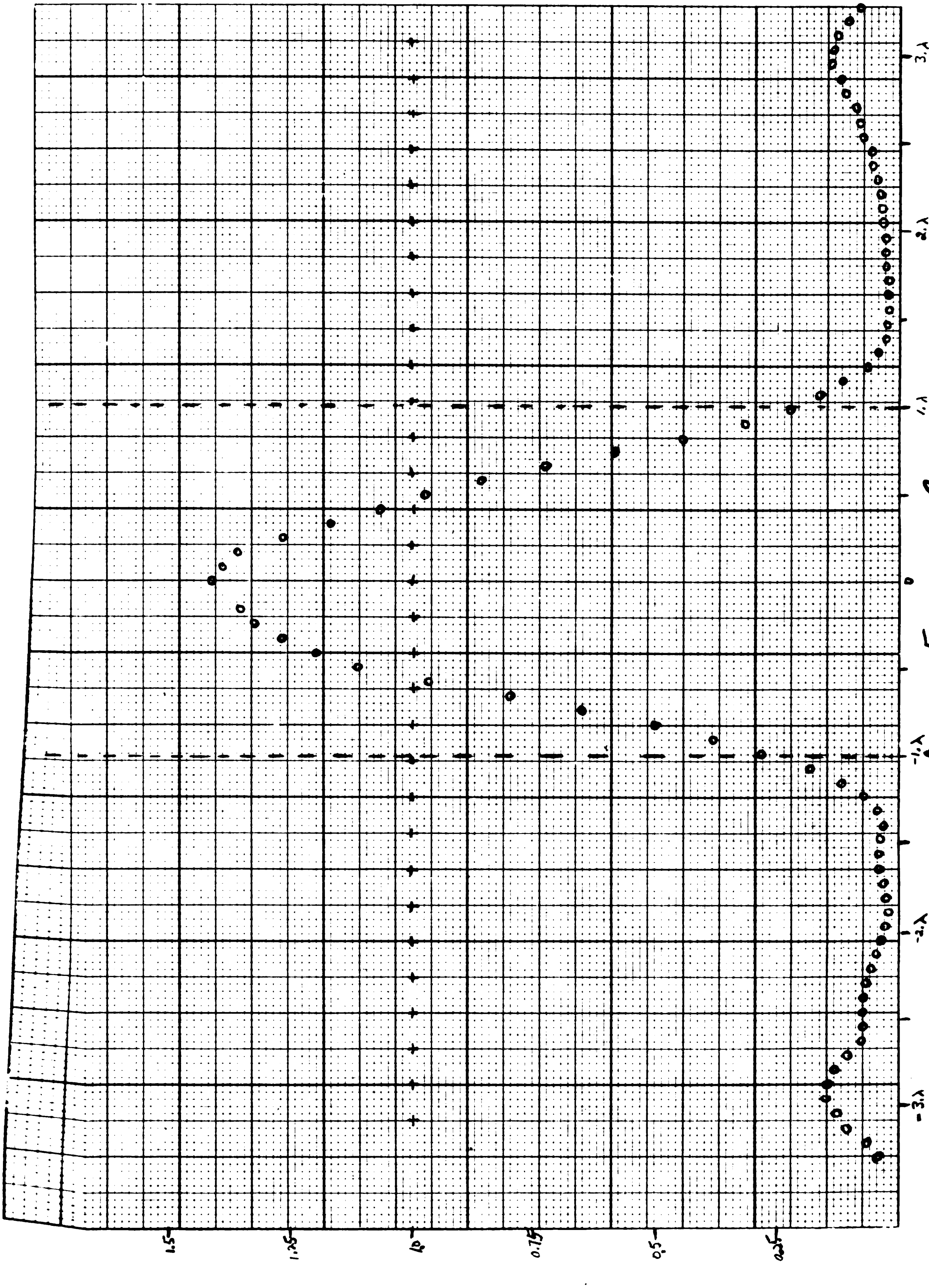

Figure 18

path a and path b is just about 1.0 wavelength, we get a low point, in the intensity distribution pattern.

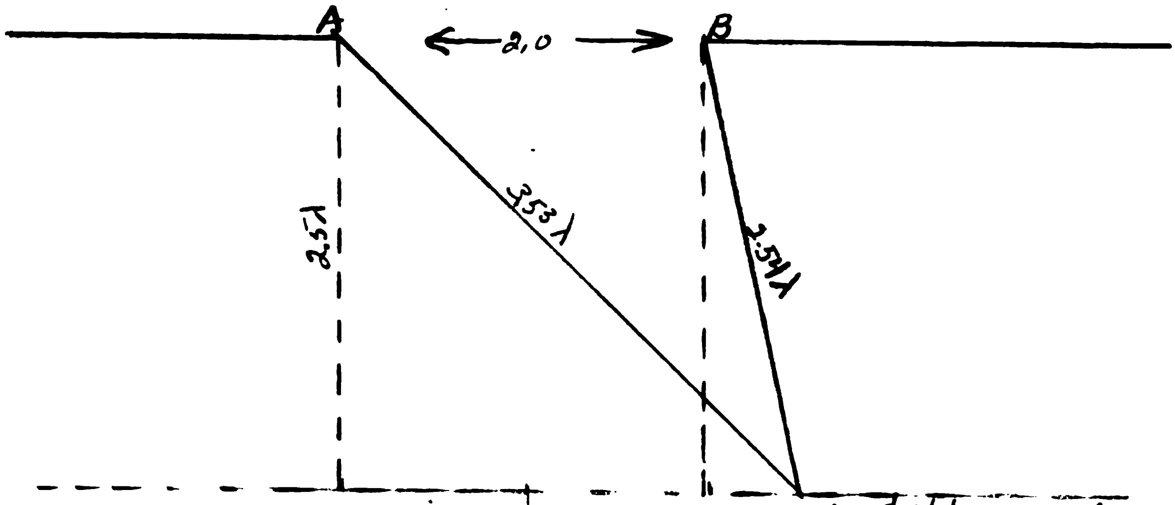

Figure 19

Evidently, that low point is not expected to reach zero, on account of the difference in amplitude between the radiation from A and the radiation from B, their paths being different.

So far, intentionally, we have neglected the distance factor $\sqrt{\frac{\lambda}{r}}$ in the intensity variations. But the influence of that factor is very low in comparison to the phase angle factor and furthermore, in some cases, it is within the experimental error. We can mention however that the distance factor might be responsible for the asymmetry of the secondary maxima about their own maximum points.

The pattern obtained with a 3 λ slit at a distance of 2.5 wavelengths, is a little more complicated for the following reasons:

a) The change in path difference being more rapid than in the previous case, we expect more frequent variations, even in the unshadowed region.

b) At any point in the unshadowed region we will have to account for three radiations, each having its own intensity, and phase.

c) We do not know the intensity at points close to $\delta = 0$

For all these reasons, we will not attempt to account for the "shoulders" appearing on the intensity pattern, on Fig. 21 . But the low point of these "shoulders" seems reasonable if one considers that, for example, at the "shoulder" B,

a) The phase angle between the radiation from the source at infinity and the radiation from edge B changes very slowly with regard to the displacement.

b) The main factor in the intensity pattern should be the phase angle between the radiation from edge A and the plane wave.

A glance at the next diagram and one sees that, at the low point of the "shoulder", the phase angle is in the neighborhood of π.

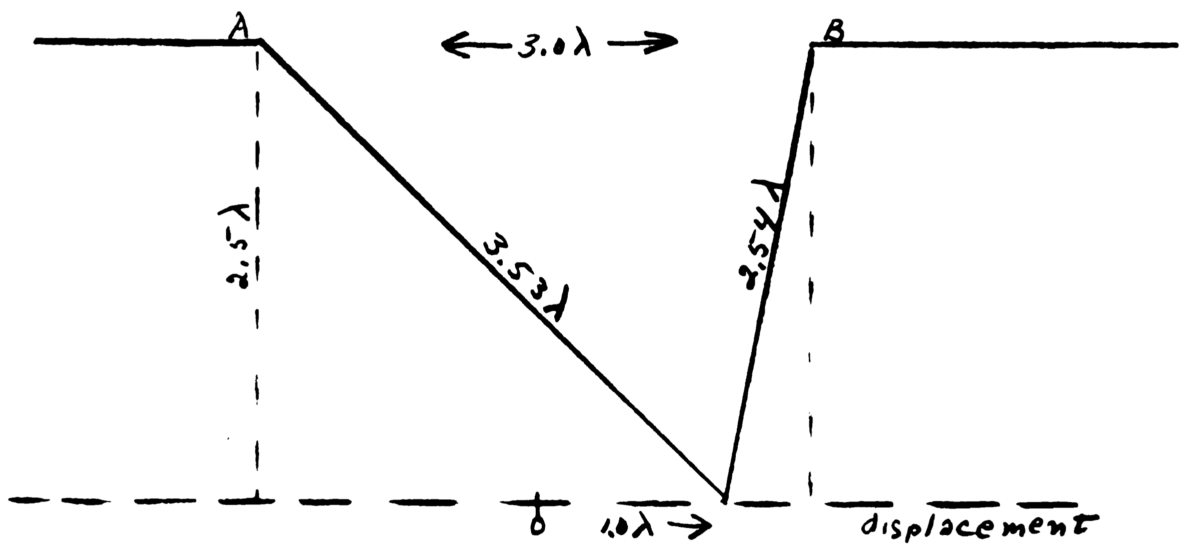

Figure 20

A similar method shows that the low point in the shadow region is again due to the phase angle π between the radiation

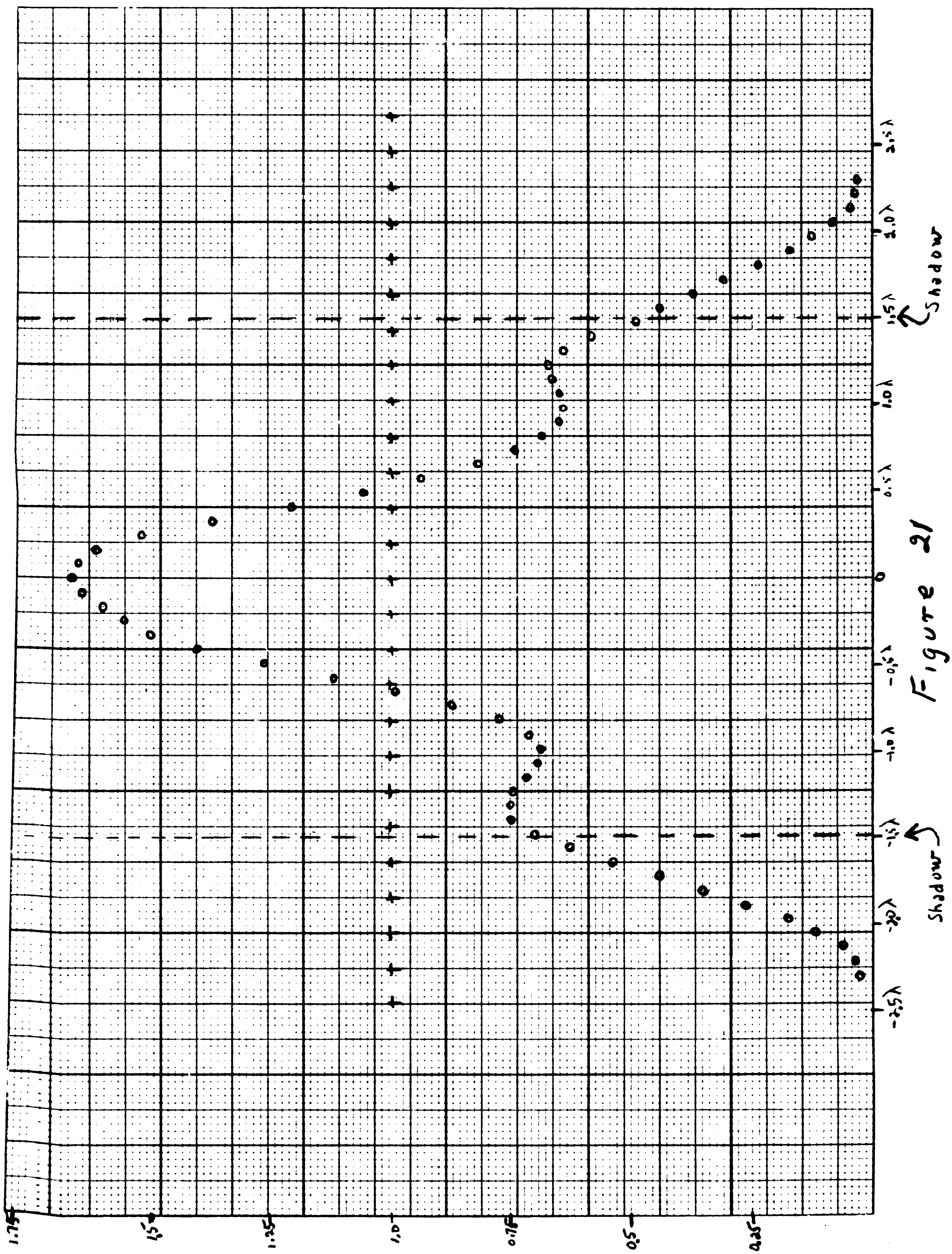
1.75
1.5
1.25
1.0
0.75
0.5
0.25
2.5λ
2.0λ
1.5λ
1.0λ
0.5λ
0
-0.5λ
-1.0λ
-1.5λ
-2.0λ
-2.5λ
Shadow
Shadow

Figure 21

from A and the one from B. That low point shows up at about 28 cm. from the central point.

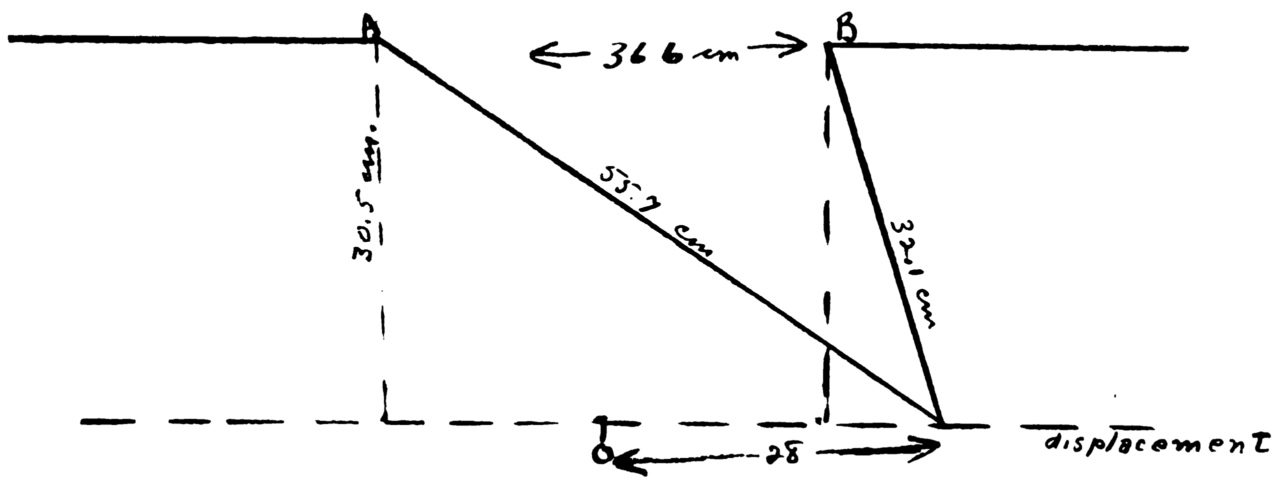

Figure 22

We have taken similar readings with a 3λ slit at a distance of 5.0 wavelengths, and the pattern is shown in Fig. 24. The same method as previously still accounts nicely for the minimum at 23.5 cm. from the central point

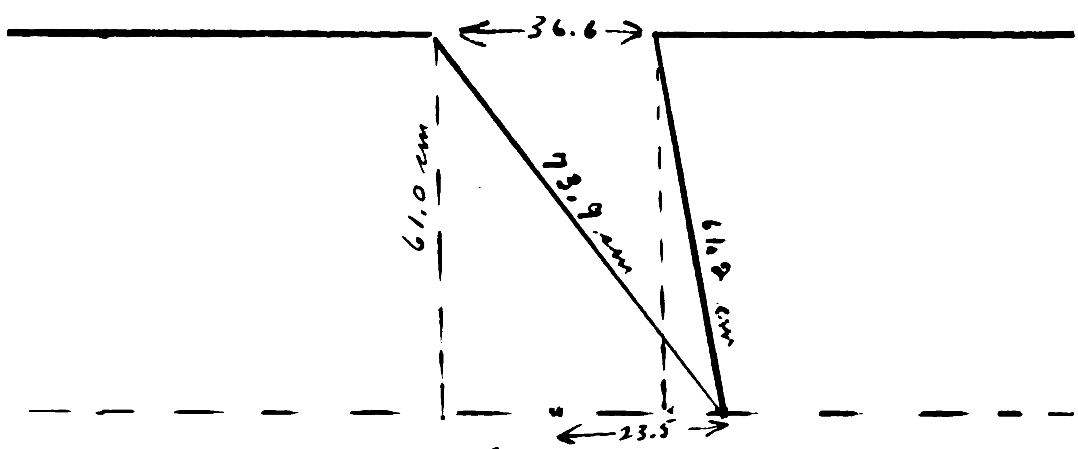

Figure 23

But one should not draw drastic conclusions from this pattern, because at this distance, the slit loses its character of "infinite slit", in height as well as in the size of the half-planes.

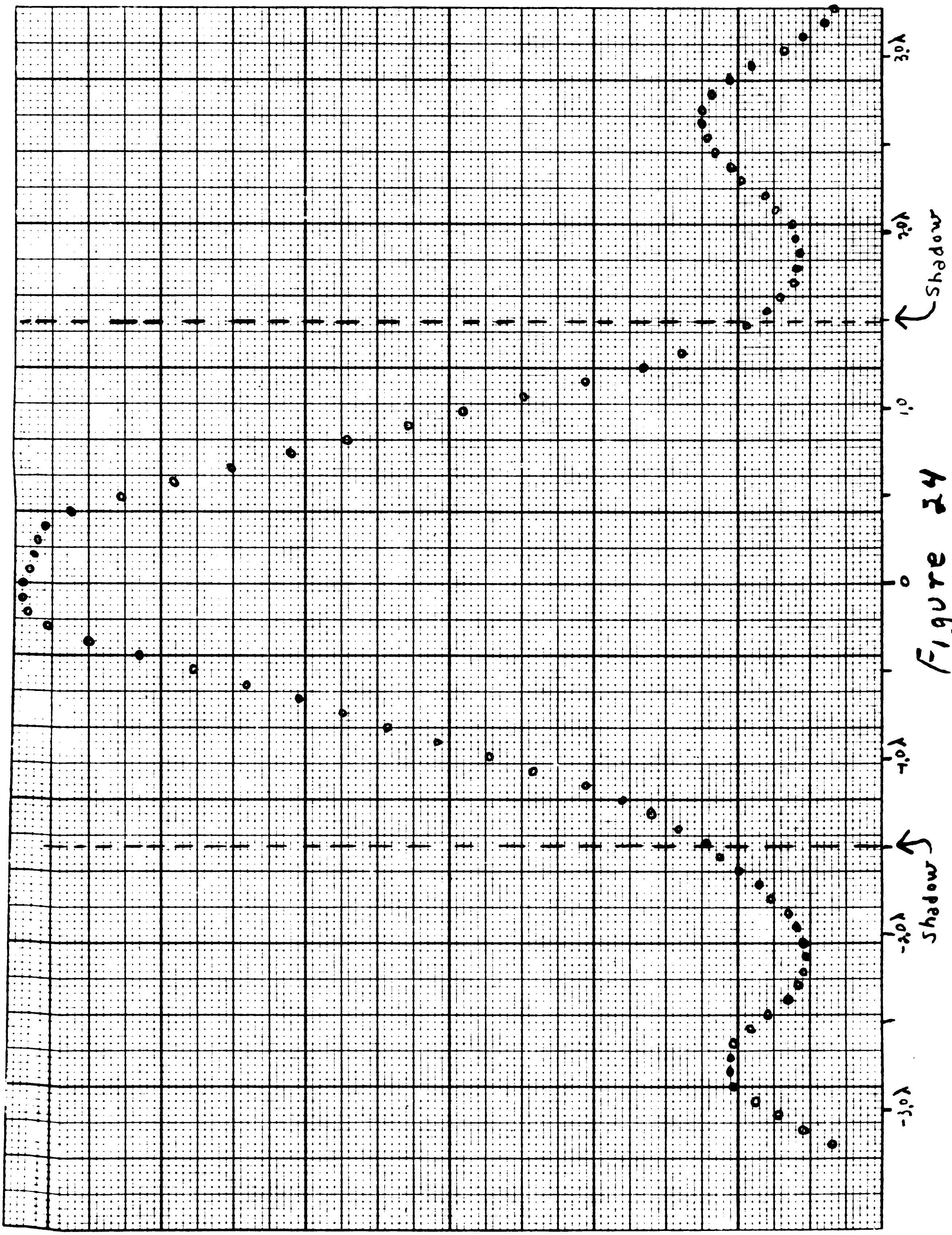

Figure 24

PHASE SHIFTS INTRODUCED BY PARAFFIN.

Up to now, we have considered all our diffraction patterns as interference patterns, the interfering radiations being from three different sources: a source at infinity and a source at each of the two edges A and B.

We have also recognized that the intensity depends upon different factors among which is the phase angle between the radiations. Now, if we cause a phase shift in any of the radiations, by introducing a medium of a different index of refraction, we should expect changes in the patterns.

But this may become much more complicated than desired. In the following, we introduce a first approach to that kind of work. And, in so doing, we have tried to make it as simple as possible.

A "slab" of paraffin was introduced in the path of two of the radiations. The pattern we should get at a distance of 2.5 wavelengths, will depend upon many different factors:

a) In place of a plane wave coming from a source at infinity, a part of our new plane wave will have its phase shifted by an angle: $\alpha = \frac{2\pi}{\lambda}(n-1)t$

where λ is the wavelength

n is the index of refraction of paraffin for this frequency.

t is the thickness of the "slab"

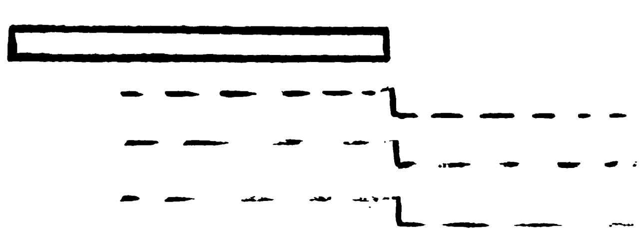

Figure 25

b) The radiation from A is also shifted by an angle:

$$\alpha = \frac{2\pi}{\lambda}(n-1)t \sec \delta$$

where δ is the angle between the radiation and the normal .

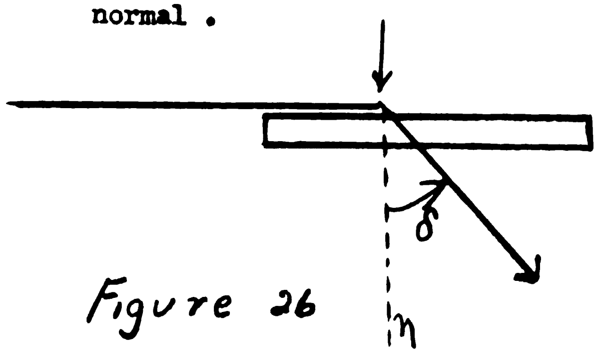

Figure 26

c) The intensity of those two radiations will be somewhat diminished because of the reflection at the two surfaces of the paraffin "slab" (change of index of refraction).

d) Furthermore, there will be a third cylindrical wave arising at the edge of the "slab" of paraffin. And, as up to now, we must admit that there is not much we can say about this last radiation.

However, the problem is simplified if :

a) we stay away for the moment from the critical point p, where there is a phase change.

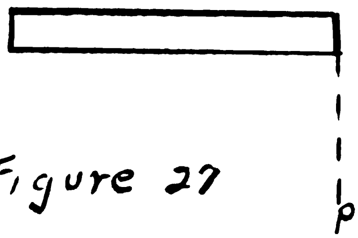

Figure 27

b) the reflection at the two surfaces of the "slab" of paraffin is neglected.

c) the third cylindrical wave arising at the edge of the "slab" is certainly very weak, in the same way and order as the reflected wave and is neglected.

Besides these small corrections then, the new problem looks the same as before except for the phase shifts.

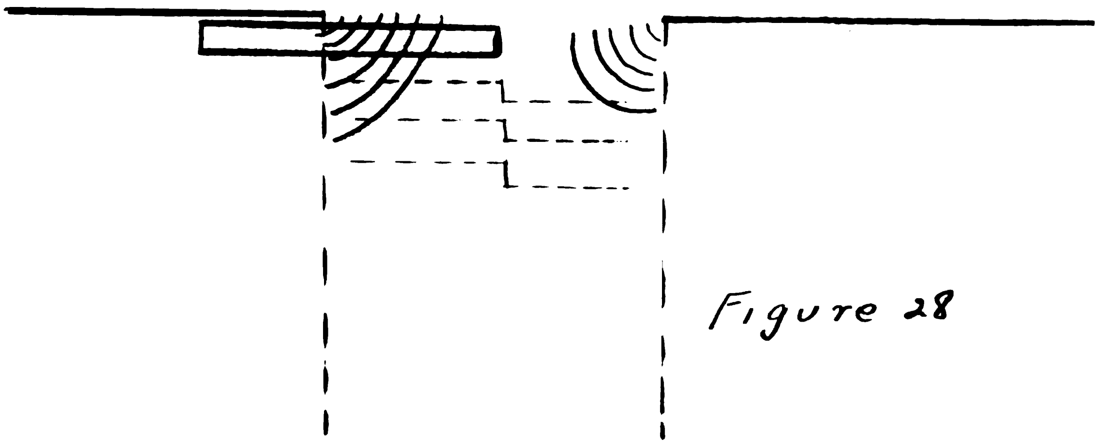

Figure 28

In the new pattern, there is one feature we can predict at once: the central maximum that we observed in almost all patterns will be shifted. Indeed, most of the time, in the unshadowed region, a maximum point will show up where the two cylindrical radiations are in phase. Since one of these radiations is now shifted in phase, most of the time one should expect to find a maximum point shifted from the center.

However, one should not try to predict accurately the place of the maximum unless we are certain of:

1) the index of refraction of the introduced medium.

2) the intensity of the transmitted radiation, through that medium.

3) the δ factor of the intensity of the radiation.

4) the exact thickness of the introduced medium.

5) and something more about the cylindrical wave arising at the edge of the "slab" of paraffin.

In Fig. 31, we have plotted the intensity distribution for two different situations: with and without the "slab" of paraffin.

Fig. 31a is for the case of a 2λ slit:

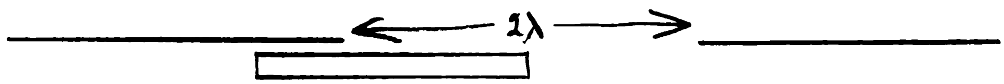

Figure 29

Fig. 31b is for the case of a 3λ slit:

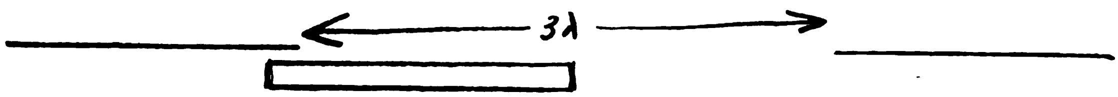

Figure 30

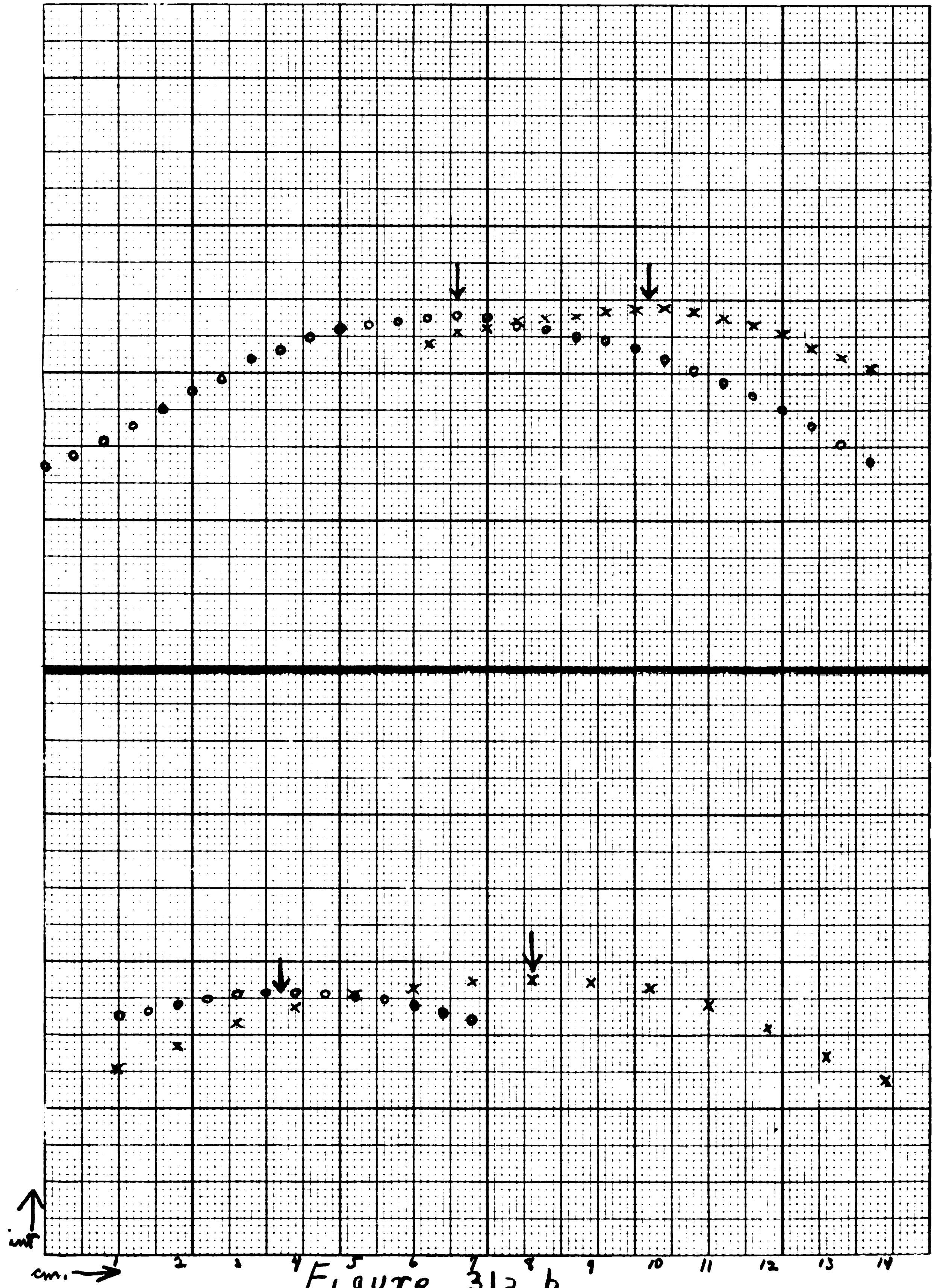

Figure 31a, b

CONCLUSION AND SUGGESTIONS.

An appreciable improvement would show up in the quantitative readings if the slit were wider: 5λ or 8λ or so. The interaction between the edges would then be considerably reduced. But at the same time, the slit would lose some of its "infinity" in height. A good idea would be to use a shorter wavelength, so that the dimension of the instruments will not become prohibitive.

There is still a lot of work to do in the region of $\delta \simeq 0$. In fact, we know that the intensity is not infinite at that point. In our interpretation we assumed a sudden change of phase for the plane wave from the source at infinity: which should give a discontinuity in the intensity distribution at that point unless there is another sudden change of phase of another radiation of equal intensity, which can only be the cylindrical wave from the edge.

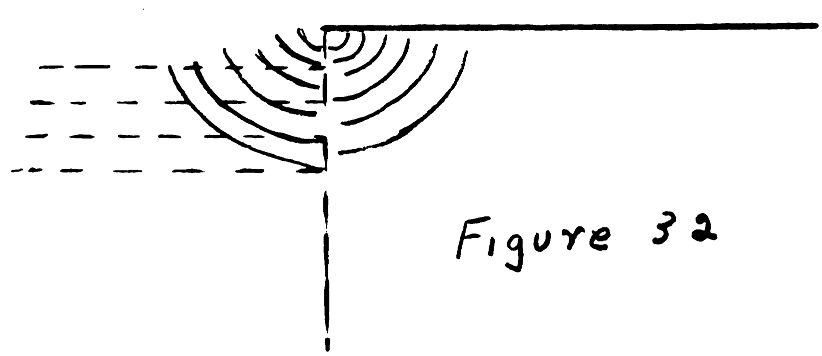

Figure 32

Another point of interest would be the study of the different radiations independently. One could then make use of the very strong polarization of the system and study independently the π and σ cases.

A rapid check in the course of our experiment showed that one can use the polarization of the system and "separate" the different radiations. The detector used as a probe, ean take three orientations: three perpendicular axes. Each orientation will eliminate any radiation propagating along that axis.

REFERENCES.

(1) Wolfsohn G. "Strenge theorie der Interferenz und Beugung." Handbuch der Physik. Vol. XX.

(2) C.L. Andrews: "Diffraction pattern of a Circular Aperture at Short Distances" in "The Physical Review" Vol. 71 June 1, 1947, p. 777

(3) C.L. Andrews: "Correction to the treatment of Fresnel Diffraction" in "The American Journal of Physics" Vol. 19, May 1951, p. 280

(4) Robert E. Houston Jr.: "The radiation pattern of circular apertures". A thesis for the degree of M.S. at Michigan State College.

(5) Charles Kittel: Introduction to Solid State Physics, p. 110

(6) S. Silver "Microwave Antenna Theory and Design" Radiation Laboratory Series. (1949).